Chapter 12
Forensic Evaluation of Long-Distance Flow in Gently Sloped Ground During the 2018 Sulawesi Earthquake, Indonesia

Hemanta Hazarika, Divyesh Rohit, Takashi Kiyota, Mitsu Okamura, Siavash Manafi Khajeh Pasha, and Sukiman Nurdin

12.1 Introduction

The Sulawesi Island of the Indonesian archipelago was struck by a powerful earthquake of moment magnitude (Mw) 7.5 on September 28, 2018, at 18:02:44 local time. The earthquake had a hypocentral depth of 20 km with epicenter at 0.256°S (latitude) and 119.846°E (longitude) in the Donggala Regency of Minahasa Peninsula, about 70 km north of the provincial capital of Palu (USGS 2018). The event had a peak intensity of 8.5 on MMI scale observed in Palu region, which experienced the devastating damage. The mainshock was preceded by a major foreshock of magnitude Mw 6.1 and followed by multiple aftershocks of magnitude Mw > 5.5 for many days. The tremors of the earthquake were felt till the Eastern Kalimantan region of Borneo Islands as well as Tawau district in Malaysia. The event triggered extensive flow-slides in ground with very gentle gradient (about 1–5%) in some areas, such as Balaroa, Petobo, Jono Oge and Sibalaya. Numerous landslides, in the coastal areas of Palu, Donggala and Mamuju, also caused tsunami. According to the National Agency of Disaster Management, Indonesia, it caused 2,101 causalities, 4438 injuries and with 1373 still missing (BNPB 2018). The

H. Hazarika (✉) · D. Rohit
Kyushu University, Fukuoka 819-0395, Japan
e-mail: hazarika@civil.kyushu-u.ac.jp

T. Kiyota
Tokyo University, Tokyo 113-8654, Japan

M. Okamura
Ehime University, Ehime 790-8577, Japan

S. M. K. Pasha
IMAGEi Consultant, Tokyo 102-0043, Japan

S. Nurdin
Tadulako University, Palu 94148, Indonesia

locations of mainshock, foreshock and aftershocks are shown in Fig. 12.1 (Hazarika et al. 2020). The data presented in Fig. 12.1 are for the duration between September 28 and October 8, 2018. The occurrence and magnitude of foreshock, mainshock and aftershocks signify the amount of energy accumulated across the Palu–Koro fault (PKF). The earthquake was triggered by the strike-slip movement of PKF which straddles the Palu city. The event created a rupture of length about 200 km in 30 s at a speed of 4–4.1 km/s, which lies in between the P and S wave propagation velocities, also termed as super-shear rupture (Bao et al. 2019).

The horizontal and vertical motions in EW, NS and UD directions are depicted in Fig. 12.2a, b along with their power spectrum recorded at the Japan International Cooperation Agency (JICA) seismological station in Palu (BMKG and JICA 2018). The measured peak ground accelerations (PGAs) in each (EW, NS and UD) direction were 199 Gals, 200 Gals and 335 Gals, respectively. The dominant frequency of strong motion is from 0.2 to 0.6 Hz, which can be attributed to many geotechnical damages.

The extraordinary and extensive large-scale flow failures in some areas of Palu city, Donggala and Sigi Regency of Central Sulawesi inflicted widespread damage to public and private infrastructural facilities including irrigation structures, houses, government buildings and bridges. Also, the event caused loss of thousands of lives, injuries to many more and thousands of missing. Balaroa, Jono Oge, Petobo
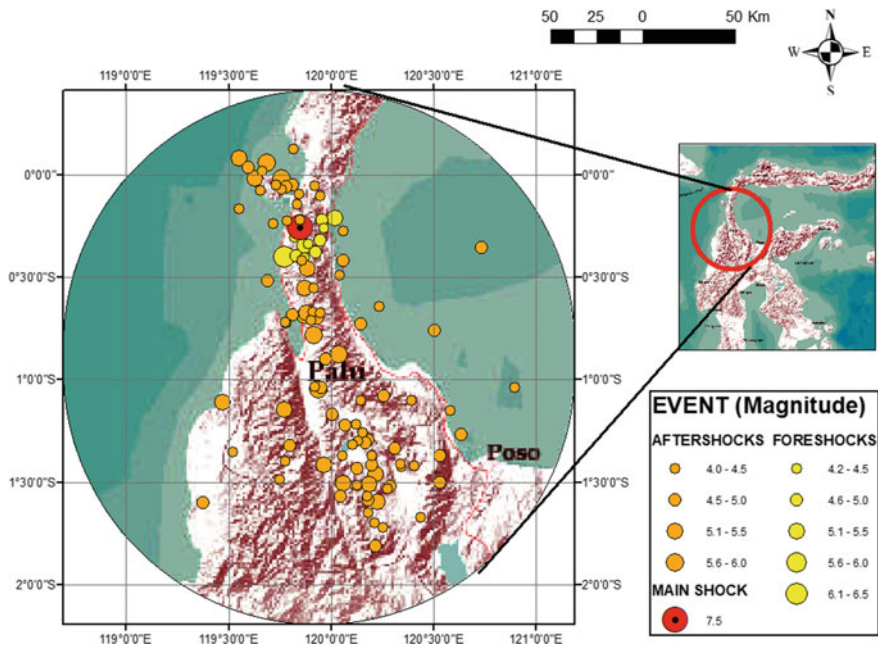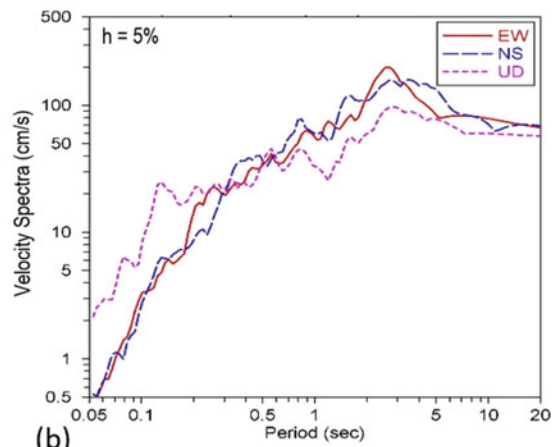

Fig. 12.1 Occurrence of foreshocks, mainshock and aftershocks with varying magnitude (Hazarika et al. 2020)

Fig. 12.2 Strong ground motion: **a** E–W, N–S and U–D components and **b** velocity response spectrum (modified from JICA report 2019)
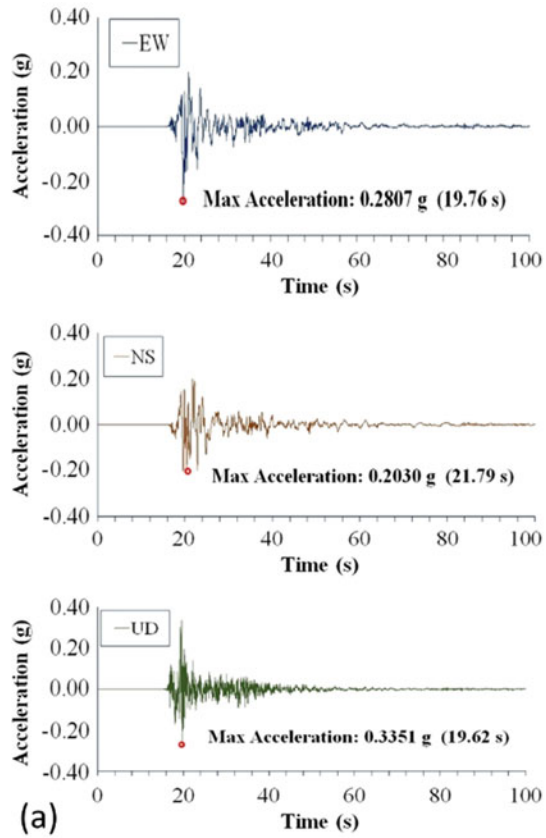
and Sibalaya of Palu city were severely affected due to the large-scale flow-slides and mud flows. It was first time in the history of recorded seismic events that such large-scale flow failures were initiated by an earthquake, sweeping away thousands of houses, and that too, in grounds with gentle gradients. According to Kiyota et al. (2020), these long-distance flow-slides were caused by multiple factors such as presence of less-permeable cap layer leading to the formation of interlayer water called water film, liquefaction of underlying sandy layer, presence of confined aquifer and overall geology of the area.

The geological as well as seismological characteristics of Central Sulawesi region, the findings from the aerial, geotechnical and geological investigations and subsequent data analyses, performed by the authors aftermath the Palu earthquake for each flow-slide site, are described in the following sections.

12.2 Geological and Seismological Characteristics of Central Sulawesi Region

Sulawesi Island has an intricate tectonic cluster that segregates the converging Eurasian, Indo-Australian and Philippines Sea Plate (Kadarusman et al. 2011; Bellier et al. 2001; Watkinson et al. 2011). Due to the intense collision and inter-action of the three plates, Sulawesi Island has multiple active faults, among which Palu–Koro fault (PKF) is the most seismically active. The sinistral PKF straddles the Palu region of the Central Sulawesi Province. On September 28, 2018, several meters of horizontal crustal displacement were observed across the PKF, which was established through satellite image analysis (Heidarzadeh et al. 2019). All the flow-slide sites were located across or near the fault zone.

The PKF with an average slip rate of 40 mm/year and an extension rate of 11–14 mm/year is the most active fault on earth, which is quite contrasting for a simple strike-slip fault (Socquet et al. 2019). The greater Palu area is surrounded by 10-km-wide mountains and lowland on eastern and western banks. The earthquake ground motions triggered four large-scale flow-slides in Balaroa, Petobo, Jono Oge and Sibalaya, with multiple resembling features in the flow-slide and the sur-rounding terrain.

The geomorphology of Palu city and vicinity is contrasting in eastern and western side of the lowland region along Palu River (van Leeuwen 2005). The underlying rocks on the eastern side are mainly Triassic to Jurassic metamorphic rocks (Palu Complex—Gumbasa Complex), while those on the western side are sedimentary rocks of the Upper Cretaceous, and there are penetrating rocks (Palu Granite/Kambuno Granite) in the underlying rocks. The plains along Palu River are overlaid by Holocene deposits of mainly alluvial fans, while the stratigraphy of the catchment area of Balaroa, Petobo, Jono Oge and Sibalaya, where the extensive flow-slides occurred, consists of granites and granitic metamorphic rocks (gneissose granite) which tend to be weathered into sandy soil with small uniformity
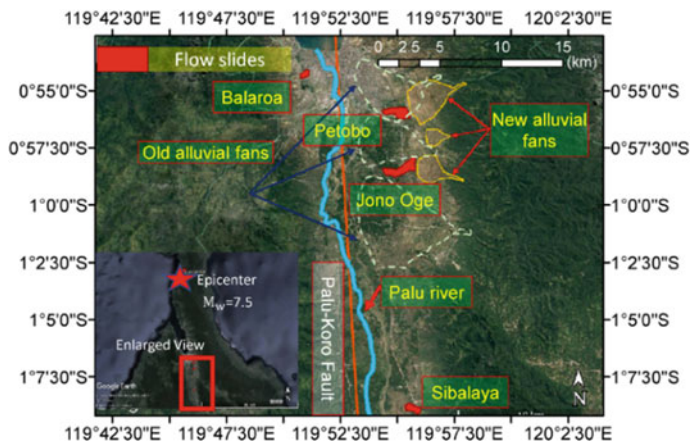
Fig. 12.3 Distribution of alluvial fans and the locations of long-distance flow-slide (marked in red) in different areas of Palu (Hazarika et al. 2020)

coefficient of particle size. Uniquely, in the western side of Palu Valley, there was no flow-slide observed with area overlain by sedimentary rocks, which are vastly distributed around the flow-slide area of Balaroa (Kiyota et al. 2020).

As shown in Fig. 12.3, the flow-slide sites are all situated along the edges of Palu Valley in the low-lying regions, where the new alluvial fans converge with the old alluvial fan deposits of Palu River (Hazarika et al. 2020). Further, according to Kiyota et al. (2020) the recent alluvial fans situated at higher elevation are comparably small and with a gradient of 5% had groundwater at lower level due to the permeable coarse gravel layers. On the other hand, old alluvial fans located at lower elevation are comparably large with a gradient of 2–5%. Due to shallow water table and easy access to groundwater, these areas have been utilized for growing paddy, with formation of some human settlements. Extensive flow-slides occurred in the floodplain with loose overlying sediment layers, located in the lowland area between the large fans.

12.3   Earthquake-Induced Flow-Slides and the Resulting Damage

Figure 12.4 shows an outline of the flow-slide consisting the collapsed part (main scarp), flow part and sedimentation part. The devastated areas have very gentle gradient with an average of 1–5%, and they are located directly below a knick line on a new alluvial fan. Furthermore, surface water was present in all the damaged areas despite scanty rainfall prior to the survey. The subsections below discuss the findings of the field investigation at all the major flow-slide sites by the three
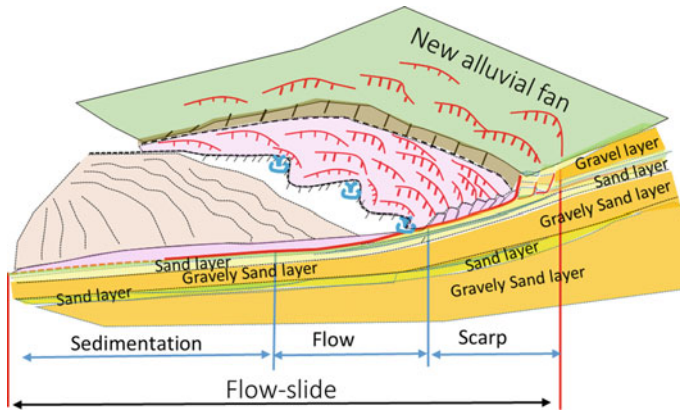
Fig. 12.4 Outline of long-distance flow-slide (JICA 2019)

research groups led by the authors from Kyushu University, University of Tokyo and Ehime University, Japan.

12.3.1 Flow-Slides at Jono Oge

Flow-slide extent and ground profile

The flow-slide at Jono Oge was the longest with respect to the debris flow and ground movement among all the flow-slides, which were triggered due to the 2018 Sulawesi earthquake. The origin of the flow-slide was observed at the crown, just besides the irrigation channel in eastern edge of Palu Valley (Fig. 12.5). The flow-slide was spread over an area of 1.5 km^2 of area with maximum displacement of 2 km. (Hazarika et al. 2020). The location of flow-slide was at the bottom of alluvial fan created at the valley mouth in the space between old alluvial fans with gentle gradient, low elevation and shallow groundwater table (Kiyota et al. 2020). The flow-slide damaged approximately 500 units of houses in the area with many being swept away or buried under the soil. It should be noted that 90% of the flow-slide area was utilized for agricultural activities. Shallow groundwater table and subsurface water in the overlying sandy layers, due to the presence of irrigation channel, probably would have aggravated the weak ground conditions and contributed significantly to the extensive flow-slides stretching over a few kilometers.

Characteristics of ground movement and soil profile.

Based on the observations made by Hazarika et al. (2020), the flow-slide profile in Jono Oge is categorized into four zones (I, II, III and IV) according to ground movement mechanism, surface features and maximum displacement (Fig. 12.6).
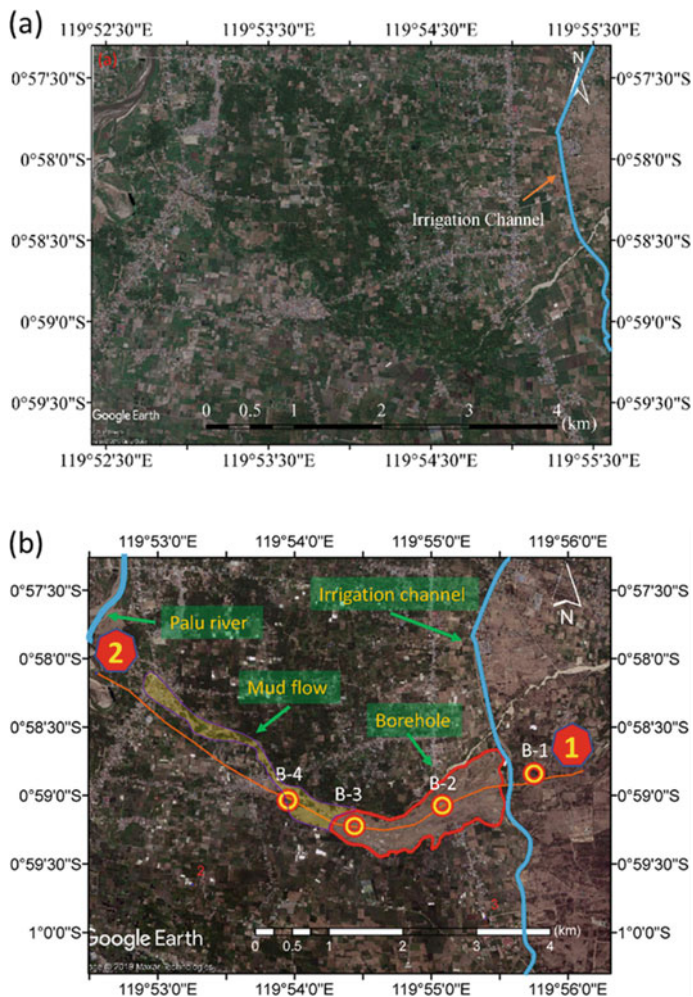
Fig. 12.5 Satellite imagery and ground profile of Jono Oge area **a** before earthquake, **b** after earthquake and **c** cross section at profile 1–2 (Hazarika et al. 2020)

Zone I includes the crown or head scarp, which extends from northeast side of failure zone (parallel to the western boundary of irrigation channel) to the southeastern side of failure zone where it meets the channel. The overlying soil strata of the main scarp were highly stratified with an alternating layer of sand, silt and organic soil as seen in Fig. 12.7a which implies the area was a wetland at the lower end of the old fan (Kiyota et al. 2020). This zone also is characterized by scouring and erosion of surface sediments due to the breach of irrigation channel which discharged large volume of the water (Fig. 12.7b). The maximum displacement of soils in this zone ranges from 2 to 50 m.
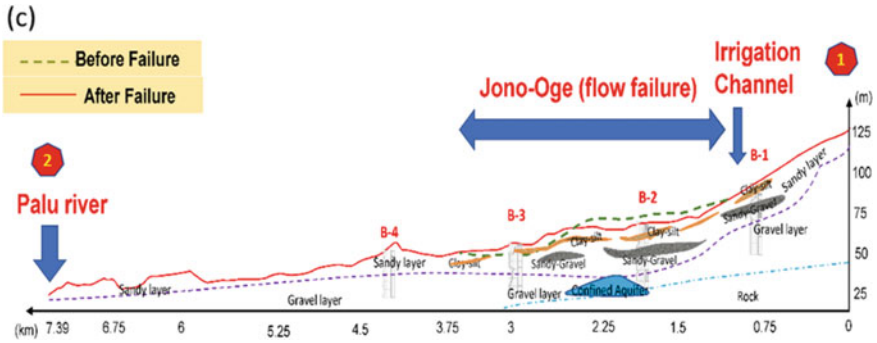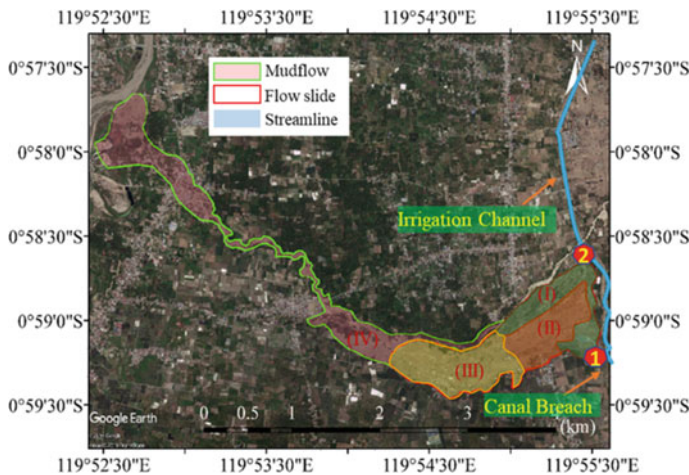
Fig. 12.5 (continued)

Fig. 12.6 Flow-slide area categorized into zones based on ground displacement in flow-slide area (Hazarika et al. 2020)

Zone II, where the flow-slide initiated after the onset of possible liquefaction in the sandy and sandy-silty layers below the ground surface, was the surface soil layers started moving toward the southwest direction of failure zone. The surface features show large extensional cracks with drastic change in soil morphology (Fig. 12.8a). Figure 12.8b shows the displacement of a house which moved approximately 1200 m due to the flow-slide. The maximum displacement in this region varies from 300 to 1300 m. The residuals of the displaced house after the cease of flow-slide can be seen in Fig. 12.8c.

Zone III is the region, where most of the disaster debris, including house rubbles and uprooted trees, got deposited. As shown in Fig. 12.8b, the debris of the structures and mudflow from Zone II piled up in the Zone III.
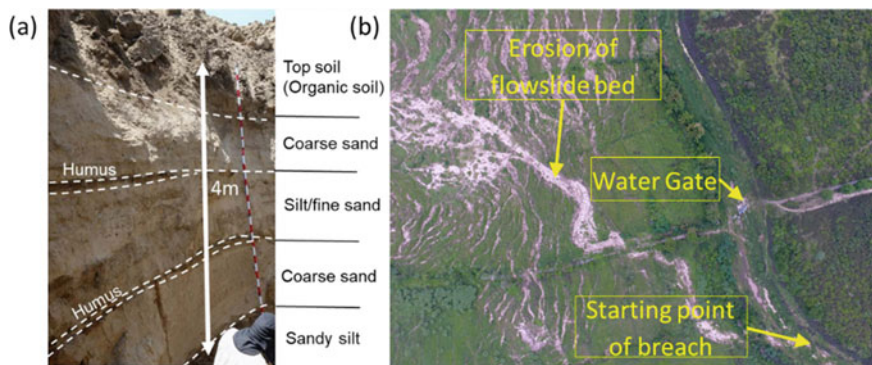
Fig. 12.7 a Soil stratification observed at the crown (Kiyota et al. 2020) and **b** UAV imagery of channel breaching and water gate destruction in Zone I (Hazarika et al. 2020)

Zone IV is located at the toe of the flow-slide and close to Palu River. The breached irrigation channel in Zone I discharged huge amount of water, which then flowed into Zone IV along with the debris. This debris flow which then confluence the stream flowing on the west bank of the flow-slide and finally ended up flowing into the Palu river (Fig. 12.9).

Damage to infrastructures

The ground motion caused damage to housing, transportation and irrigation structures. The damage due to flow-slide in Jono Oge was further aggravated due to the breach of irrigation channel, as shown in Fig. 12.10, which shows the completely dry state of the channel. According to eyewitness, the embankment of the irrigation channel breached 2 min after the earthquake, which implies that the damage to the embankment of irrigation channel was not caused by the earthquake motion, but it might have been caused by the dragging force due to flow-slide.

According to another eyewitness, living near the downstream of the flow-slide, after the ground motion ceased, the thick mud water flowed down for approximately an hour, and the houses along the river bank were inundated with the mud and debris, as shown in Fig. 12.11. From the mud inundation mark on the houses, it could be deduced that the height of mudflow at the downstream area was about 7 m above the current river water level. It is to be noted that such mud slide was not observed in other areas, such as Petobo and Sibalaya, where similar damage occurred in the irrigation channels. The origin of the water that caused the flood in Jono Oge could be attributed to a confined aquifer beneath the affected area of flow-slide (Kiyota et al. 2020).

In situ tests

In order to evaluate the probable mechanism and progression of long-distance flow-slide at Jono Oge, the research team from Kyushu University performed in situ tests using the portable dynamic cone penetrometer test (called hereafter PDCPT) at

Fig. 12.8 Zone II **a** surface deformation with extensional cracks, **b** displacement of house structure from Zone II to Zone III due to the flow-slide and **c** residues of the displaced house after the flow-slide (Hazarika et al. 2020)
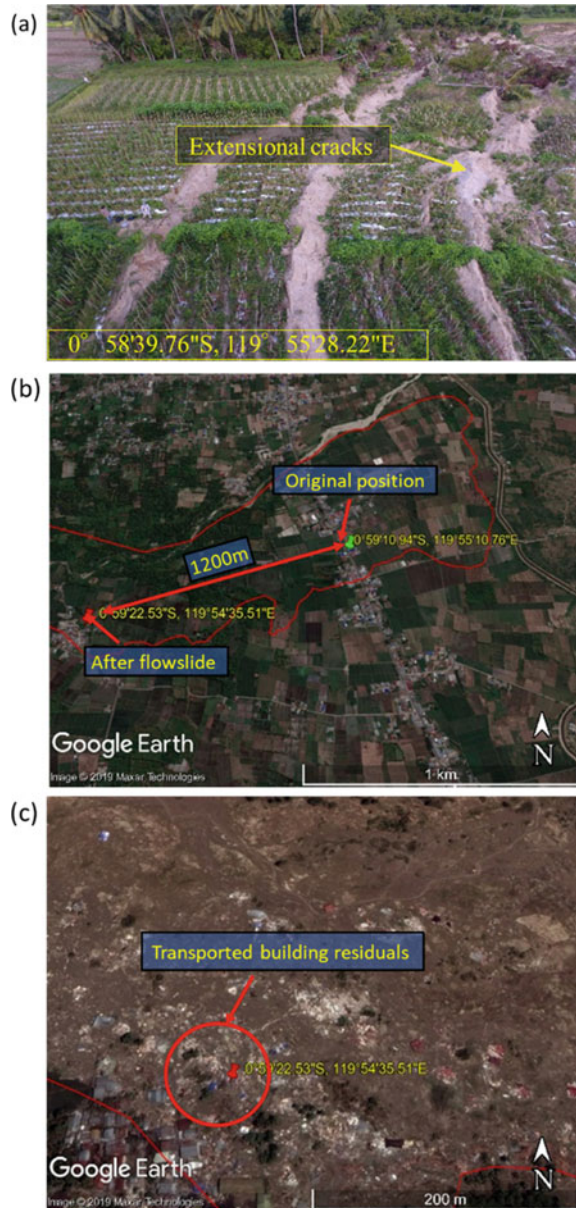
multiple locations in and outside the failure zone. One test (PDCPT1) was conducted outside the flow zone, and the other tests (PDCPT2 ∼ 8) were conducted inside the flow-slide zone in two arrays, to assess the subsoil profile in two different directions as shown in Fig. 12.12 by two dotted lines.
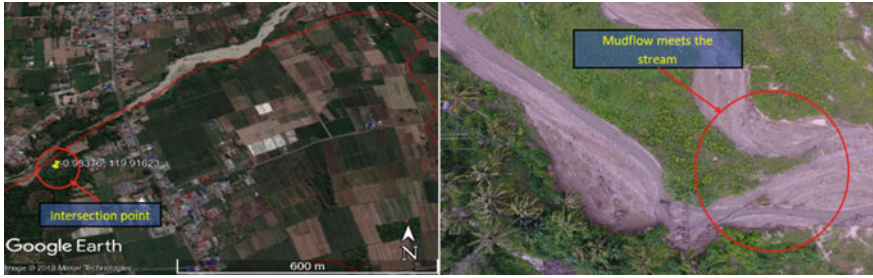
Fig. 12.9 Intersection of mudflow and stream (Hazarika et al. 2020)

Fig. 12.10 Damage to
irrigation channel and control
gate in Jono Oge

Fig. 12.11 Mud inundation mark on the house depicting the height of mud flow passing the area
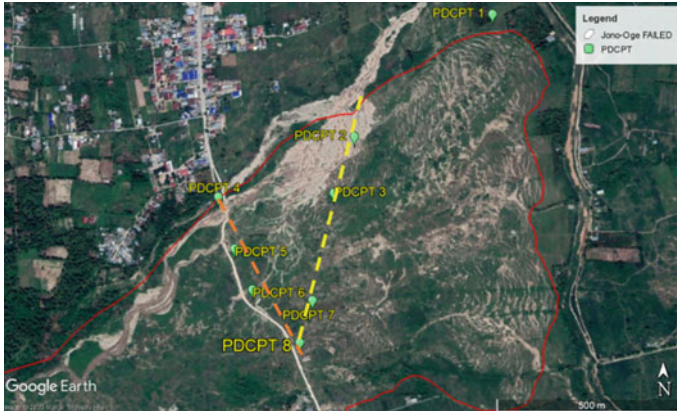(Kiyota et al. 2020)

Fig. 12.12 Locations of the PDCPT and collected soil samples at Jono Oge (Hazarika et al. 2020)

Figure 12.13 represents the plot for converted N_{SPT} value versus depth for PDCPT1 at the location, which is outside the failure zone, far from extensional cracks. As observed in Fig. 12.13, there is a decrease in the N value for the soil layers below 2.5 m, indicating the presence of loose liquefiable layers. The risk of liquefaction is also high due to the presence of groundwater table at a shallow depth (water level at the time of testing G.W.L = 2.3 m). Furthermore, to correlate the soil lithology at location PDCPT1, a pictorial image of the cliff nearest to the extensional crack is shown in Fig. 12.14. As shown in Fig. 12.14, the overlying layer consists of 10–20 cm of organic soil, followed by 30–40 cm of clay and silty clay layer, while the underlying 10–20-cm-thick silty sand layer is sandwiched between the upper clayey layer and lower 10–20-cm-thick clayey silt layer.

Fig. 12.13 PDCPT conducted near the crown of flow-slide and the test result (modified from Hazarika et al. 2020)

Fig. 12.14 Profile of exposed soil layer due to the extensional cracks near PDCPT1 (Hazarika et al. 2020)

Furthermore, beneath the silty layer, there were several layers of sandy and gravelly sand, which appeared to be influenced by probable liquefaction in the underlying layers (Hazarika et al. 2020).

The PDCPTs 4, 5, 6 and 8 were conducted alongside the damaged road as discussed before in Fig. 12.13. PDCPT4 was conducted beside the collapsed bridge near the stream (Fig. 12.15a). PDCPT5 was conducted within the flow-slide Zone (I) near the reconstructed road as shown in Fig. 12.15b. PDCPT6 was conducted in the Zone (II) alongside the reconstructed road as depicted in Fig. 12.15c. PDCPT8 was conducted few meters away from the red house which experienced no displacement during the flow-slide (Fig. 12.15d). The results of the PDCPTs conducted are converted in terms of SPT N values and are plotted alongside the locations of the tests (Fig. 12.15a–d). Here, in Fig. 12.13a, the overall soil profile up to the depth of 5 m shows weak soil, and this was due to its presence near the river, where the bridge collapsed during the earthquake. As seen from the test results, the N values for all the locations are less than 10 up to a depth of 2.5 m which signifies very loose to loose soil below the ground surface. It can be observed in PDCPT 8 that the soil below 4 m is of medium strength as against those observed in PDCPTs 4, 5 and 6. The deposits at the PDCPT locations are believed to be loosely deposited sand and silty sand layers which were carried over from the upstream of flow-slide region (Hazarika et al. 2020).

The red house shown in Fig. 12.15d was the only structure that did not move from its original location, as compared to all other structures in the flow-slide region. This could be attributed to the massive mat foundation over which the house was built. The self-weight of the mat foundation along with the house restrained its
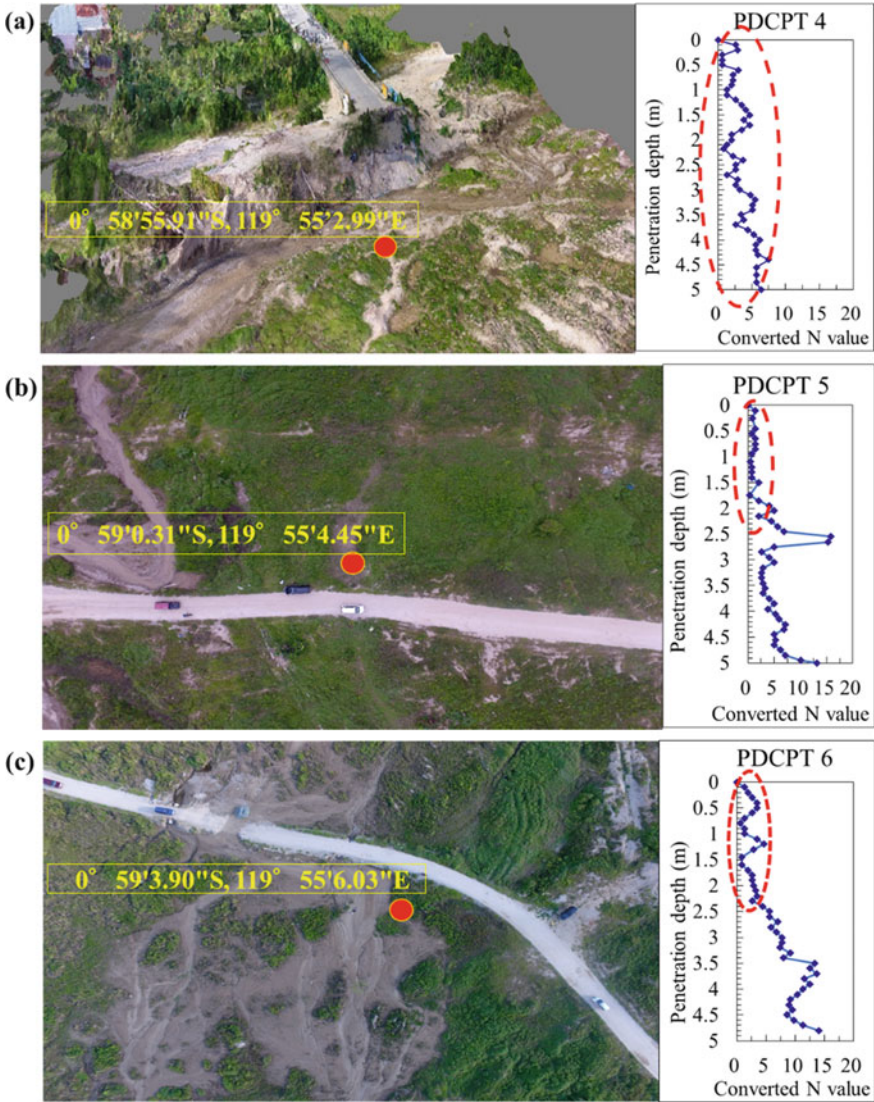
Fig. 12.15 Aerial imagery of PDCPT locations and converted SPT N value versus depth (modified from Hazarika et al. 2020)

lateral displacement even though some structural elements of the house were partially damaged due to the impact of debris. Figure 12.16 displays the aerial view of the unmoved red house along with other houses, which moved from few meters to few hundred meters.
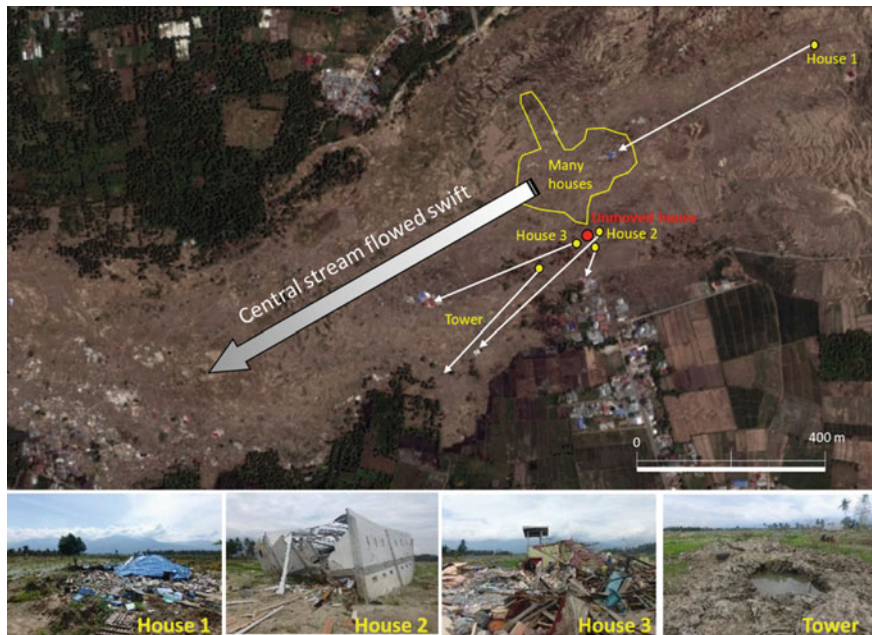
Fig. 12.15 (continued)

Fig. 12.16 Displacement of housing structures in the flow-slide zone in Jono Oge (Kiyota et al. 2020)
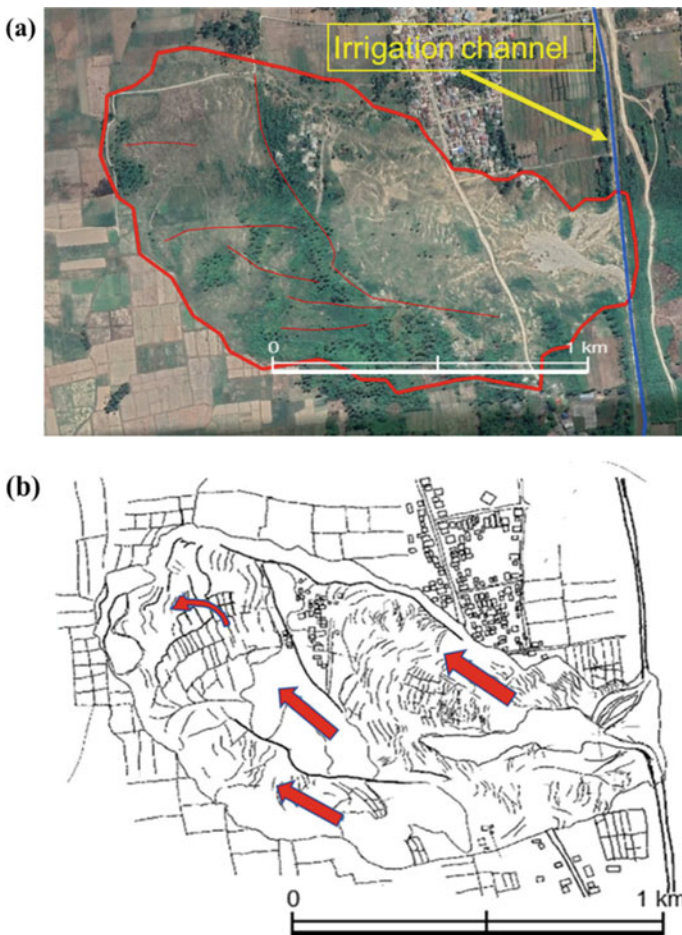
12.3.2 Flow-Slide at Sibalaya

**Flow-slide extent and ground movement**

The failed area of flow-slide in Sibalaya is situated on the east side of Palu Valley, 18 km south of Jono Oge area. The watershed of the failed area is approximately

5.3 km^2. Here, the flow-slide took place at the bottom of alluvial fan at the valley mouth. The alluvial fan at the higher elevation has a steep slope of about 8%, while, in the region of flow-slide, the slope gradient is approximately 4% in the upper part and 2% in the middle and bottom parts. Figure 12.17a shows the Google Earth image of the flow-slide in Sibalaya after the earthquake. The flow-slide area could be divided into three zones, and each zone flowed 200–400 m in the northwest direction from their respective positions (Fig. 12.18b). Sibalaya has an irrigation channel above the main scarp, which suffered significant damage similar to the ones in Jono Oge and Petobo.

The normal strain contour map of the ground movement shown in Fig. 12.18a provides a quantitative description of overall ground displacement characteristic. As

Fig. 12.17 Flow-slide at Sibalaya, **a** area after the earthquake as captured by the UAV and **b** ground movement during the flow-slide in different zones (Kiyota et al. 2020)
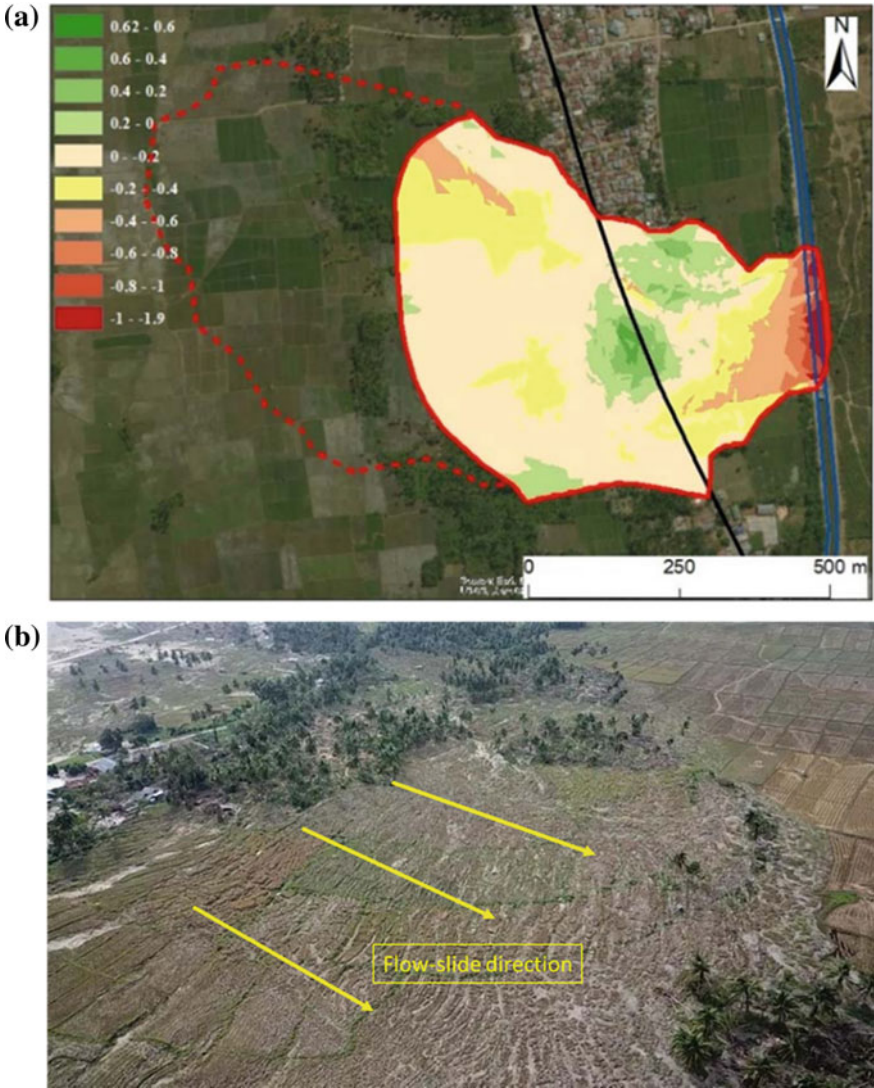
Fig. 12.18 Sibalaya flow-slide region: **a** normal strain in east–west direction, ε_x, and **b** flow-slide direction and extensional cracks in downstream zone (Okamura et al. 2020)

observed from the figure, extremely large tensile strain is generated in the narrow zone of the upstream region. Similarly, in the upstream region (paddy fields), which is just below the crown or main scarp, the tensile strain ranges from 20% to 60%. In this zone, all the houses and roads, along with paddy fields and trees, were displaced by about 350 m. In contrast, the tensile strain is relatively small in the area between the upstream and downstream paddy fields, including the original road that

was passing through this area, and compressive strain was observed (Okamura et al. 2020). Here, the negative tensile strain implies that the ground moved downstream from its original position causing extensional cracks, while the positive tensile strain relates to the compression of existing soil surface due to thrust from accumulating or depositing soil mass from upstream. The aerial view of flow-slide direction showing the extensional cracks in the downslope region of the flow-slide is shown in Fig. 12.18b.

According to the findings of Okamura et al. (2020), the flow-slide occurred across a region of approximately 534,700 m^2, in which around 339,200 m^2 of area subsided and 195,500 m^2 heaved. The overall volume of subsidence and heaving is 609,900 m^3 and 745,900 m^3, respectively, which was evaluated from the terrain survey of the flow-slide region during the site investigation and the elevation profile of the region available from various sources. The average ground subsidence across the failure region is 0.25 m, while the area outside the edge of the flow-slide subsided by about 0.013 m.

Terrain profile of the flow-slide region

Okamura et al. (2020) conducted terrain survey of the flow-slide zone and generated AW3D digital elevation maps with a 0.5 m resolution to analyze change in topography of region due to the flow-slide. The AW3D digital elevation maps were developed with the help of Remote Sensing Technology Center of Japan, and the maps were constructed using satellite imageries acquired by Geo-Eye-1 and WorldView-1, 2, 3 and 4.

The terrain elevation from the AW3D maps is shown in Fig. 12.19a–f. In all the figures, the chainage of the irrigation channel is shown by a vertical dashed line set at 1340 m. Figure 12.19a–c shows the ground elevation profile along the flow-slide mainstream (section A–A') before and after the earthquake. Figure 12.19d–f shows the terrain elevation profile, ground slope and change in height of the flow-slide zone across sections A–A', B–B', C–C' and D–D'. All the sections were parallel to each other. It can be implied from Fig. 12.19a–c that the flow-slide caused an abrupt change in terrain elevation and slope profile in the damaged area. Also, the change in height (subsidence and upheaval) was caused due to the tension and compression strain in ground, as discussed before. Although the topographies of all these sections prior to the earthquake were similar, the post-earthquake deformations were significantly different. This could be attributed to the spatial variability of soil lithology, the mechanical properties of soils and the location of groundwater table.

Soil lithology of the flow-slide area

To understand the geological profile of the failure zone, multiple trenches were excavated in Sibalaya to examine the soil lithology and arrive at probable cause of the failure. Figure 12.20 shows the soil profile from one such trench located within the failure zone (refer Fig. 12.17a). As shown in Fig. 12.20, the subsurface soil lithology is highly stratified with layers of sandy gravel, silty sand and clay, sandy gravel and sandy soil. The silty sand and clay layer, which is sandwiched between
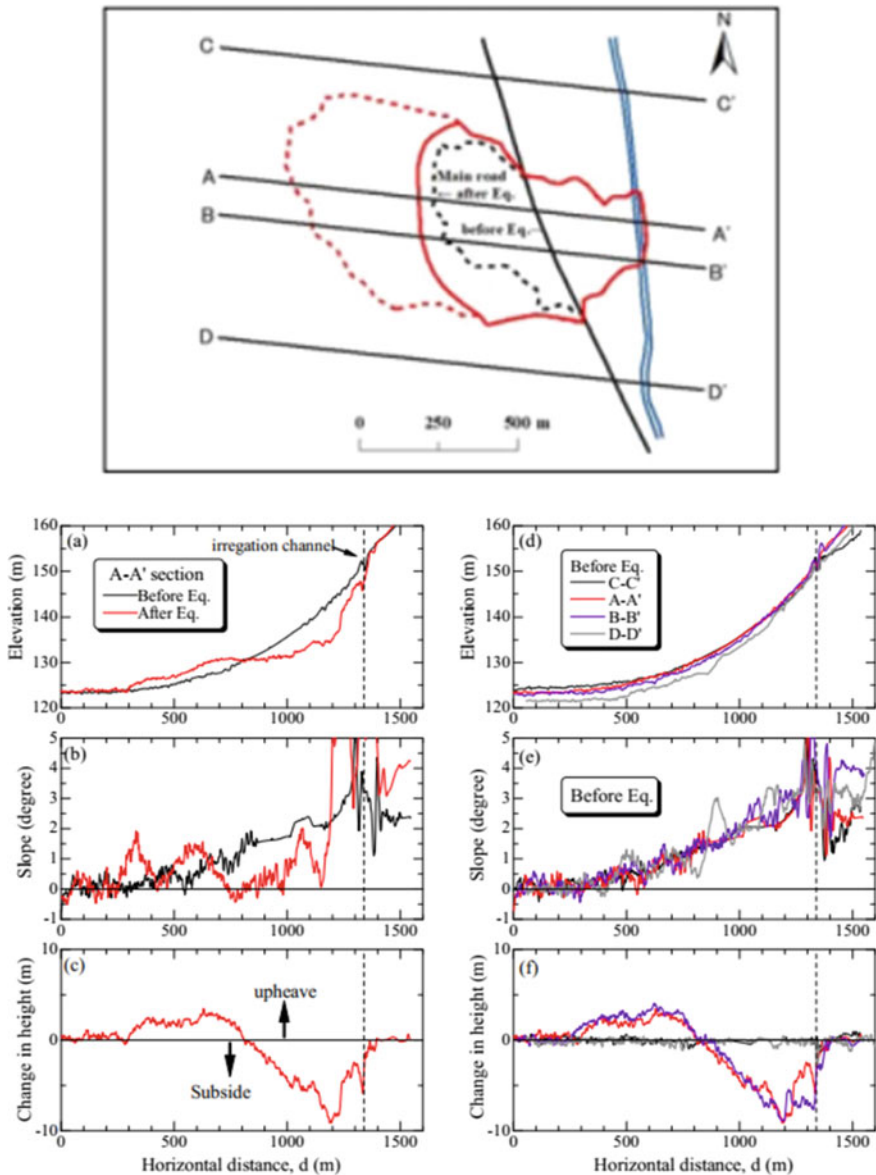
Fig. 12.19 Surface terrain characteristics parallel to the flow-slide (Okamura et al. 2020)

sandy gravel layers, is assumed to be the cause of failure by trapping the excess pore water pressure developed during the ground motion and thereby destabilizing the underlying sandy layers.
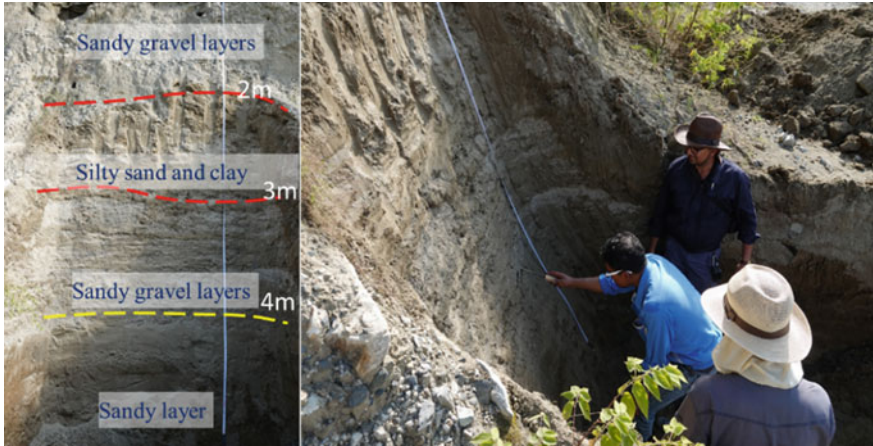
Fig. 12.20 Soil profile observed near the main scarp of failure in Sibalaya

The research group from Ehime University conducted multiple trench excavation in the flow-slide zone in Sibalaya, to study the subsurface soil profile, the locations (indicated as #1 ∼ #7) of which are shown in Fig. 12.21. This subsection will discuss the findings from one particular trench referred here as Trench #1.

Figure 12.22a–d shows the images of the excavated Trench #1 as well as soil stratification. Figure 12.22a shows the aerial view of the excavated trench, while
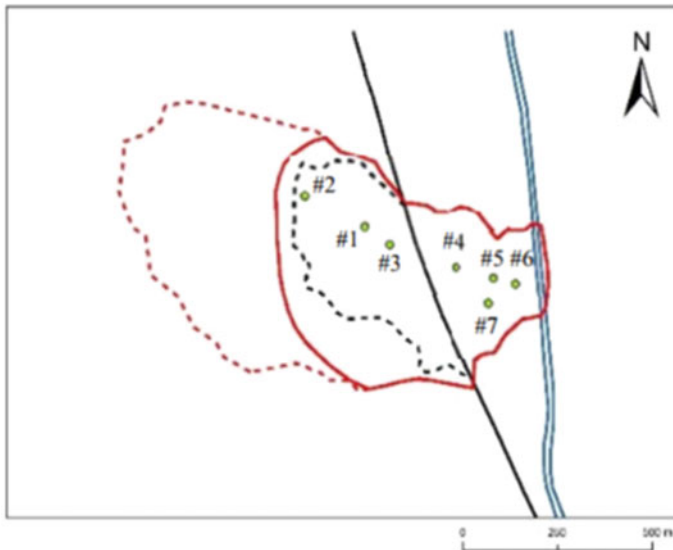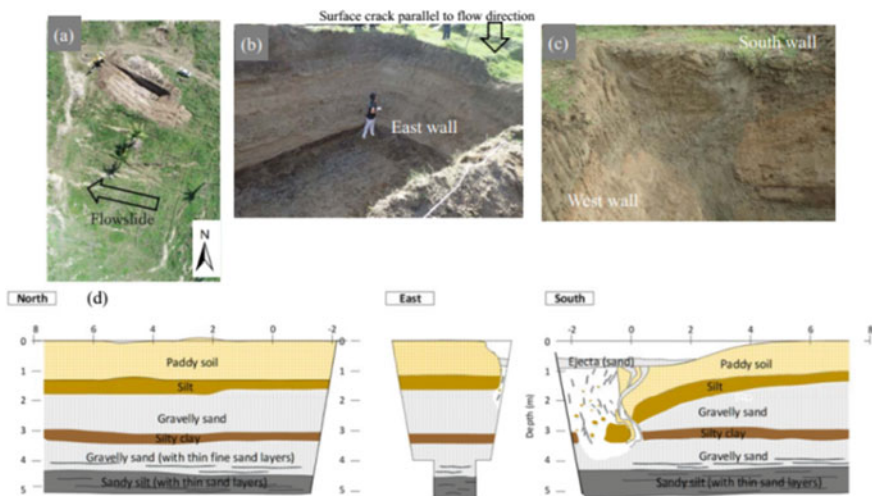

Fig. 12.21 Locations of excavated trench in Sibalaya (Okamura et al. 2020)

Fig. 12.22 Details of Trench #1 at Sibalaya. **a** Aerial photograph, **b** north and west walls in the trench, **c** southeast corner in the trench and **d** sketch indicating stratification of soil layer exposed on the walls (Okamura et al. 2020)

Fig. 12.22b, c shows the faces of east wall and west wall of the trench. The sketch of the north, east and west walls of the trench, depicting the soil profile, is shown in Fig. 12.22d. The trench was located upstream, about 150 m downslope of the irrigation channel. The longitudinal axis of the trench was oriented parallel to the flow-slide direction. In Fig. 12.22d, the gravelly sand layer underlying the surface layers is confined by multiple sand and sandy gravel layers of 10–30 cm thick, with some sandwiched silty sand layers, whose thicknesses are of the order of 10 cm. In the south wall, the surface of gravelly sandy layer sinking toward the southeast corner implies the potential liquefaction of this layer during the earthquake. Beneath the gravelly sand layer, there exists a thin stiff silty clay layer that separates the two gravelly sand layers, which seemed to be intact except at the corners. The underlying gravelly sand layer was mostly uniform, with only a few thin interlayers near its bottom. It has been observed that, in all the exposed walls, the typical configuration of non-liquefied gravelly sand layer was a stack of sand and sandy gravel layers in every 10–30 cm, with thin silty sand layers having thicknesses of the order of 10 cm sandwiched in between. This implies the potential liquefaction of both the upper and lower gravelly sand layers, resulting in shearing, which was observed in the lower gravelly sand layer.

Interview of eyewitnesses

Okamura et al. (2020) conducted interviews of multiple residents living near the flow-slide area, who witnessed the flow-slide event (Fig. 12.23a). All the inter-viewees confirmed a strong ground shaking that continued for 10–20 s, which is in accordance with the ground acceleration recorded at the observatory near Balaroa.
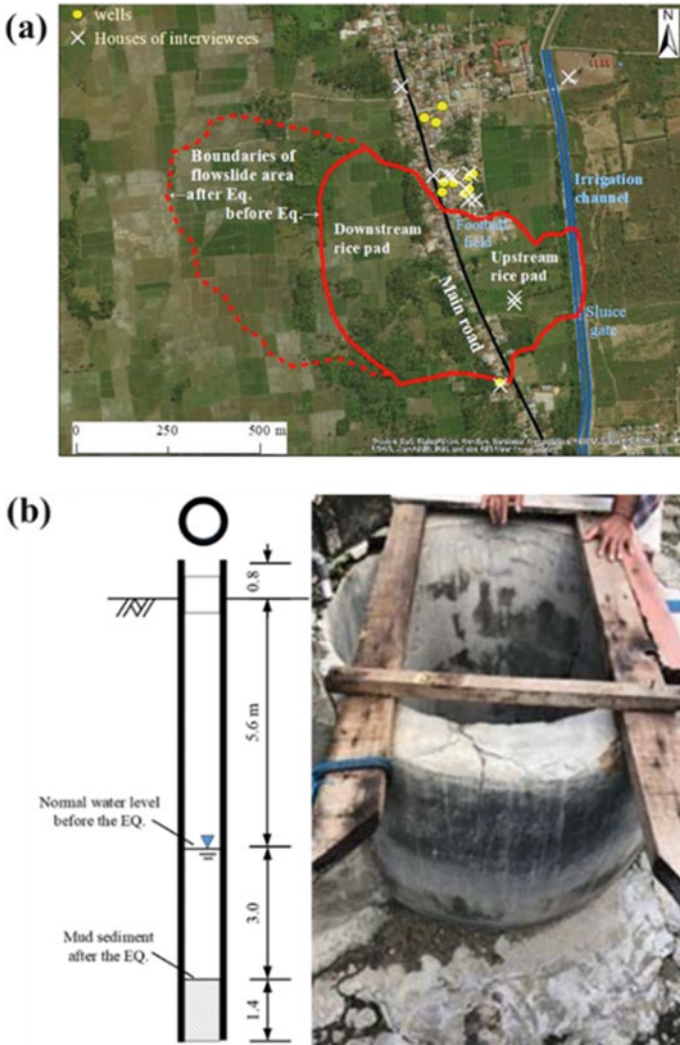
Fig. 12.23 Sibalaya flow-slide zone, **a** satellite image before the earthquake with locations of houses of interviewees, surveyed wells, main road, irrigation channel and flow-slide-affected area and **b** image and schematic diagram of well (Okamura et al. 2020)

Soon after the shaking ceased, within 10 s, almost all the interviewees felt a sudden drop in elevation. This vertical displacement, after the mainshock, was not recorded by the accelerometers near Balaroa, but was felt by many residents near the flow-slide areas on the east side of the Palu River, including residents of Sibalaya as well as Petobo and Jono Oge (Mason et al. 2019).

Thereafter, within a minute, almost all the interviewees said to have heard an extremely loud sound, similar to structural collapse or thunder. Concurrently, eight

interviewees residing near the flow-slide area observed that houses and coconut trees were moving downslope toward the Palu River at a rate faster than the average walking speed, which continued for about a minute. Multiple interviewees claimed to have seen that the water from the breached irrigation channel was flowing downhill, immediately after the ground motion stopped. All these events occurred within few minutes.

Historically, the level of groundwater table is a key in earthquake damage investigation and evaluating the liquefaction potential of ground. The research team of Ehime University also interacted with the owners of the existing wells in the area. One of the owners of a well with internal diameter 1 m and tip elevation 10 m below ground level (Fig. 12.23b) confirmed that the water level in the well before the earthquake was around 5.6 m below the ground surface, which varied minimally throughout the year. Just after the earthquake, the owner observed water overflowing from the well, which lasted for two days, after which the water level gradually reduced and finally dried up in the next couple weeks.

12.3.3   Flow-Slide at Balaroa

Flow-slide extent and ground movement

This subsection constitutes the summary of outcomings from the field survey conducted by the research team of University of Tokyo. In Balaroa, the flow-slide area was smaller as compared to Jono Oge and Sibalaya. The failed area in Balaroa was spread to about 40 ha, located on the west side of Palu Valley. The watershed area of the damaged area is approximately at 4 km^2. The failure occurred at the base of alluvial fan formed near the valley mouth, where there was no presence of discharged water at the time of survey. The maximum displacement of flowed object observed in Balaroa was about 300 m. The ground inclination before the flow-slide was very gentle (3–5%), although it was steeper as compared to those in Petobo, Jono Oge and Sibalaya. Also, in this area no irrigation channel existed.

A satellite image of Balaroa flow-slide area after the earthquake is shown in Fig. 12.24a, while the ground movement direction denoted by arrows is shown in Fig. 12.24b. The soil profile at the crown was found to be coarse sand deposit of thickness 3–4 m which was covered under debris of granite boulders. Sand ejecta from the lower layers were found in the surface layer which was covered from the upstream debris. A significant amount of ground subsidence was found near the crown of the flow-slide, while most of the overlying soil and structures moved in the east direction forming large tensile cracks. The ground subsided by an average depth of 3–4 m in the upper region of the flow-slide, while in the lower region, the ground was uplifted by 5 m, which could have been due to the accumulation of soil blocks and structural debris. Unlike Jono Oge and Sibalaya, Balaroa was a densely populated area, where around 1300 units of houses were destroyed. The presence of
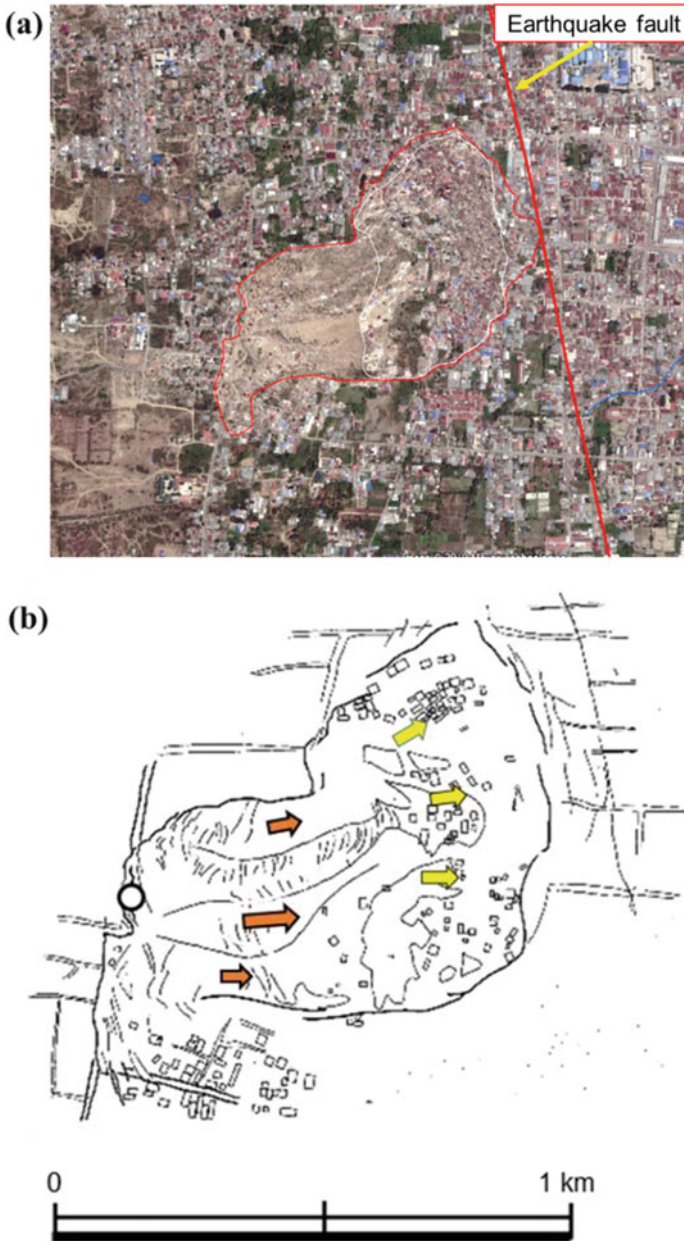
Fig. 12.24 Flow-slide in Balaroa area: **a** satellite image and **b** the direction of ground movement (Kiyota et al. 2020)

spring water inundation on the surface was found in the middle portion of the flow-slide during the survey (Fig. 12.25).

Multiple eyewitness accounts describe the movement of ground in the form of fluidized flow downhill, carrying along the houses and mosques (Fig. 12.26) with it. Also, a clear evidence of sand ejecta on the ground surface was found during the survey, and that confirmed the authors' hypothesis that liquefaction took place in the underlying soil layers (Fig. 12.27).

Furthermore, the residents of this area confirmed that the groundwater table was shallow. The presence of a confined aquifer could also be confirmed by a well digger, who observed that the groundwater sprouted to a height of 0.5–1 m, on inserting a water pipe until 6 m depth from the ground.

Fig. 12.25 Soil profile observed at the crown (Kiyota et al. 2020)

Fig. 12.26 Inundation of water after the earthquake and destroyed mosque structure due to the flow-slide (Kiyota et al. 2020)

Fig. 12.27 Sand ejecta observed in the upper part of the flow-slide (Kiyota et al. 2020)

12.3.4 Flow-Slides at Petobo

Flow-slide extent and ground movement

In this subsection, assessment of the damage, based on the survey conducted by the research team of the University of Tokyo, is described. Petobo is located on the west side of Palu Valley. It had a flow-slide area of about 180 ha. The watershed area of the failed region is approximately 14 km^2. The ground failed at the bottom of alluvial fan formed near the valley mouth. Figure 12.28a depicts an aerial image of the post-earthquake flow-slide zone in Petobo, using Google Earth along with the locations of the PDCPTs ①～④ conducted in the area. The ground displacement vectors during the flow-slide can be seen in Fig. 12.28b. The ground inclination of the failed site was very gentle (2–3%). Similar to Jono Oge and Sibalaya, Petobo also had an irrigation channel passing directly above the flow-slide area, which was damaged (Fig. 12.29). The water from irrigation channel disappeared after the earthquake. The ground movement in this area occurred mainly in two directions, as evident from Fig. 12.29.

The surface soil profile at the crown shown in Fig. 12.30 depicts the presence of alternating layer of silty sand and gravelly soil, which runs parallel to the ground surface. The soil deposits shown in Fig. 12.30 are assumed to be from the deposits caused by flow-slide. Similar to other flow-slide sites, many tensile cracks were observed in upstream slope of the flow-slide in Petobo. The ground elevation was found to be lowered by an average of 5 m.

Similar to Balaroa, Petobo was also a densely populated area, where approximately 1920 housing units were reportedly damaged due to the flow-slide. Contrastingly, the housing structures outside the boundary of flow-slide zone were
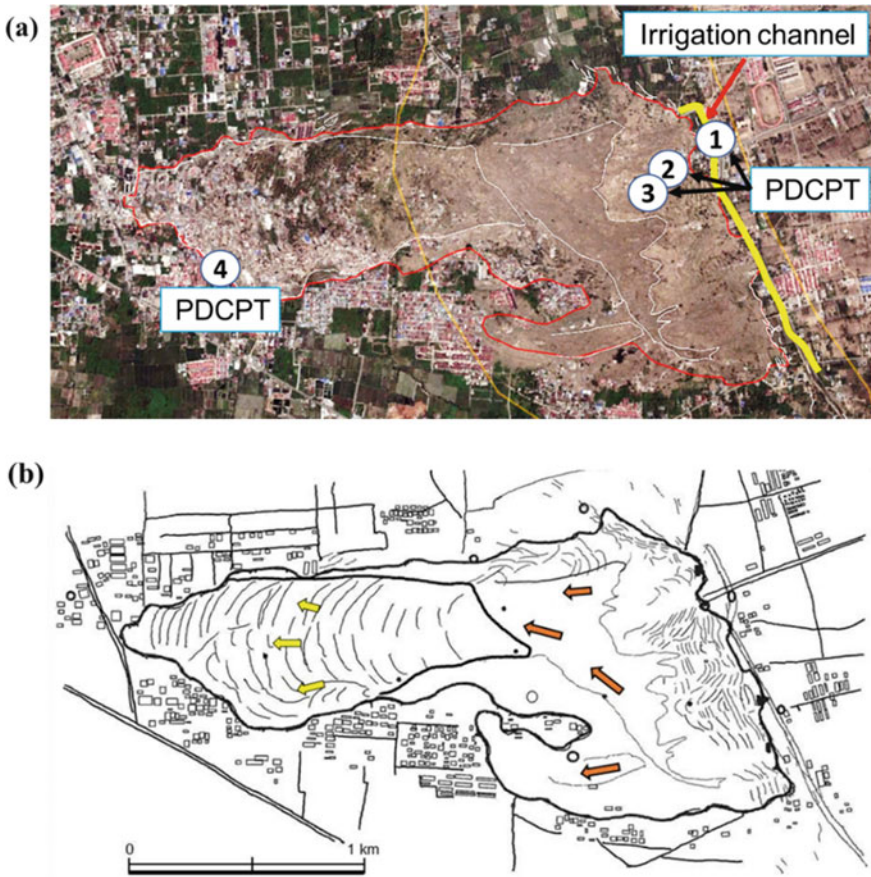
Fig. 12.28 Petobo area after the earthquake: **a** satellite imagery after the earthquake along with the location of PDCPTs ①~④ (Google Earth, 2018) and **b** ground displacement during the flow-slide shown by arrows (Kiyota et al. 2020)

not damaged, as shown in Fig. 12.31, where undamaged structure stands near the damaged structure. Housing structures which moved downstream were buried by thick soil mass and other debris (Fig. 12.32). As observed in Balaroa, the presence of surface flow of water due to formation of small springs was seen in Petobo too. Additionally, similar springs were found in the downstream sedimentation zone, which experienced about 5 m increase in its elevation, probably due to compressive strain from surrounding soil. The presence of springs at the site implies the presence of a confined aquifer (artesian water) below the ground surface. Similar to Balaroa, in Petobo too sand ejecta were observed.

Fig. 12.29 Damage to the embankment of irrigation channel (Kiyota et al. 2020)

Fig. 12.30 Soil profile observed at the main scarp of flow-slide in Petobo (Kiyota et al. 2020)

In situ tests

As described before in Fig. 12.28a, PDCPTs ①∼④ were performed in and around the flow-slide zone to evaluate the subsoil strength and condition. It is to be noted that the sand ejecta were found near PDCPT nos. ②, ③ and ④. As shown in Fig. 12.33, the subsoil condition was weak with N_{SPT} values for the PDCPT that are small which implies very weak soil deposits. It can be inferred that a combination of weak soil and shallow groundwater with artisan pressure led to the occurrence of liquefaction due to the earthquake.

Fig. 12.31 Damaged and undamaged structures (Kiyota et al. 2020)

Fig. 12.32 Spring water inundation on the ground surface (Kiyota et al. 2020)

12.4   Probable Flow-Slide Mechanism

Due to complex mechanism of failure and nonidentical geological conditions at some of the flow-slide locations, the exact mechanism of the flow-slides due to the 2018 Sulawesi earthquake cannot be clearly predicted at this stage. Furthermore, owing to the total destruction and displacement of the top soil due to the flow-slide,
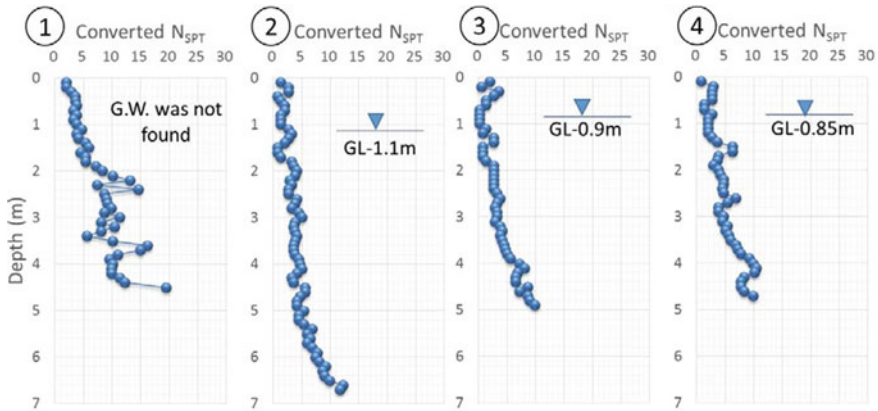
Fig. 12.33 Converted N_{SPT} values from PDCPT performed at Petobo (Kiyota et al. 2020)

added to the change in morphology, and the absence of historic geotechnical or geological data of the locations, it is difficult to arrive at the exact cause of the flow-slide at this stage and suggest a concrete hypothesis for the failure mechanism.

The flow-slide in Jono Oge initiated a minute after ceasing of the earthquake. The flow-slide carried away soil blocks with overlying houses and trees downstream toward the Palu River. The initial movement of ground occurred in Zone II, due to which the surrounding soil lost its retaining support and started moving gradually in the primary zone. The soil blocks, houses and trees were displaced by a distance of few meters (Zone I) to around 1.5 km (Zone II). Furthermore, the breach in irrigation channel caused mudflow into the already subsided area of the flow-slide. A similar case of flow failure was reported in the Lower San Fernando Dam during the 1971 San Fernando earthquake, during which the failure occurred after around 1 min of cessation of the ground motion (Bolton 1987), although the ground displacement of this huge magnitude was not observed. While, in the case of Lower San Fernando Dam, the inertia force is mainly considered as the triggering force due to the slope profile of the ground, this cannot be attributed to the flow-slides in Palu, due to gentle gradients of the areas.

Further, the subsoil lithology in Jono Oge was found to be highly stratified with fine silty and clayey sub-layers sandwiched between coarse sandy layers. These sandwiched layers acted as low-permeable capping layers trapping the liquefied sandy soils and prevent those from reaching the ground surface, thereby causing failure in the underlying soil layer. A similar case of stratified silty sub-layers was observed during the investigation aftermath the 1964 Niigata earthquake, where lateral flow up to maximum 10 meters was observed in gently sloped ground (Kishida 1966).

Low-permeable cap layer hypothesis has been studied in past through model tests by various researchers (Kokusho 1999; Kokusho and Kojima 2002; Kokusho 2015). The model tests exhibited the formation of a thin 'water film' beneath the cap layer, due to liquefaction of the underlying sand during earthquake loading. The water film is formed due to the low permeability of overlying layer which inhibits the dissipation of excess pore water pressure developed in the underlying permeable sandy layer. The water film thus formed reduces the shear strength of the underlying sandy soil layer to less than the initial static shear stress. This leads to lateral flow in a very gentle gradient under the influence of gravitational force until a static equilibrium is achieved.

In consistent with previous studies and the soil stratification observed in this forensic investigation, Hazarika et al. (2020) have proposed a hypothesis explaining the combined effects including typical geology and terrains, and water film formation under the capping layer due to liquefaction of the sandy layer, and existence of underlying artesian aquifer could be a possible reason for such long-distance flow-slide (Fig. 12.34). At this stage, no general mechanism of failure could be hypothesized for all the sites.

On the other hand, hypothesis proposed by Kiyota et al. (2020) suggested that the artisan pressure from the underlying confined aquifer triggered the flow-slide by reducing the shear strength of the overlying ground surface as shown in Fig. 12.35. Although the authors could not confirm the presence of such an aquifer yet, the JICA (2019) report confirmed the presence of a confined aquifer at a depth of 30 m through borehole tests, which is much deeper than expected. Also, the highly stratified subsoil lithology with alternating layers of sand, silt, gravel and organic soils reduced the effective permeability of the surface layers. The low permeability of surface layers inhibited the dissipation of excess water pressure, in spite of the upward pressure exceeding the critical hydraulic gradient contributed by the confined aquifer.
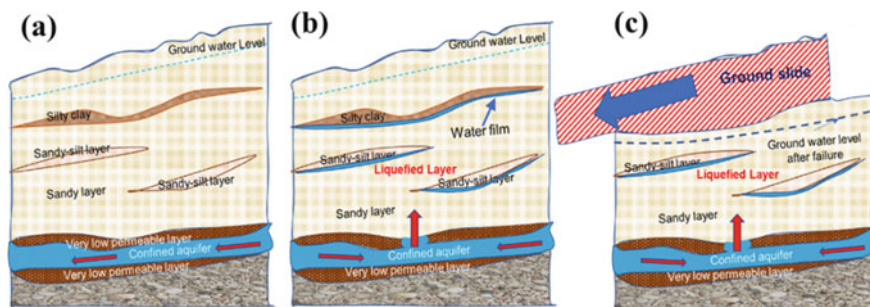
Fig. 12.34 Mechanism of flow-slide and development of water film under low-permeable layers **a** before the earthquake, **b** immediately after initiation of liquefaction and **c** after the earthquake (Hazarika et al. 2020)
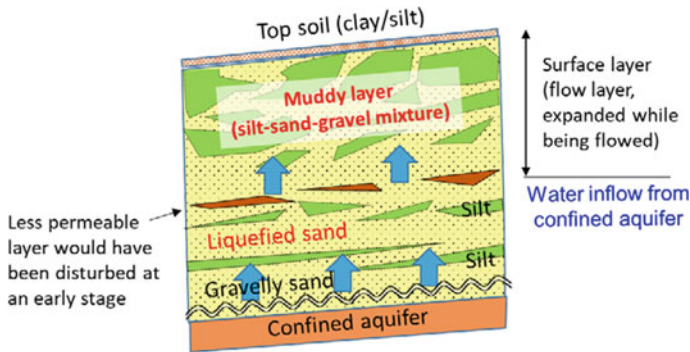
Fig. 12.35 Schematic illustration of long-distance flow-slide based on water inflow from confined aquifer (Kiyota et al. 2020)

12.5 Concluding Remarks

This paper presents a summary of the field reconnaissance conducted by the authors on the geotechnical and infrastructural damage caused by the 2018 Sulawesi earthquake. Key findings from the site investigations of all the flow-slide sites in Palu, performed by three individual research teams from Kyushu University, University of Tokyo and Ehime University, are reported in this paper. The teams collected various information using survey equipments, such as GPS device, cameras and UAV. In addition, trench surveying and in situ testing such as PDCPT and soil sampling (both disturbed and undisturbed) were conducted to investigate the ground conditions in the affected areas.

Based on the forensic analysis performed by the authors, the following conclusions could be drawn.

- The complex geology of Central Sulawesi as well as magnitude and intensity of the extreme event caused by Palu–Koro fault had significant contribution in severity and extension of geotechnical failures, such as liquefaction-induced flow-slides.
- Considering the geological features of Central Sulawesi region, it can be concluded that all major flow-slides in Palu Valley occurred at the locations, where the new alluvial fans meet the old alluvial fans.
- Complex mechanism of long-distance flow-slide at Jono Oge can be explained using interlayer water film theory due to the presence of low-permeable layers (silt and clay) over loosely deposited sandy and sandy gravel layers. Furthermore, damage in underlying artesian aquifer during the earthquake may also have contributed to the development of water film and liquefaction-induced flow-slide on the layers with very low mobilized shear resistance (nearly zero).

Further research, focusing on geophysical tests as well as laboratory tests (such as triaxial test and torsional shear test), and physical modeling are required to arrive

at the actual mechanism of such flow failures and to suggest preventive measures against future geohazard risks in the areas having similar geological features.

References

Bao H, Ampuero JP, Meng L, Fielding E, Liang C, Milliner CWD, Feng T, Huang H (2019) Early and persistent supershear rupture of the 2018 magnitude 7.5 Palu earthquake. Nature Geosci 12:200–205

Bellier O, Sebrier M, Beaudouin T, Villeneuve M, Braucher R, Bourles D, Siame L, Putranto E, Pratomo I (2001) High slip rate for a low seismicity along the Palu-koro active fault in central Sulawesi (Indonesia). Terra Nova 13(6):463–470

Bolton SH (1987) Design problems in soil liquefaction. J Geotech Eng 113(8):827–845

Hazarika H, Rohit D, Pasha SMK, Masyhur I, Arsyad A, Nurdin S (2020) Large distance flow-slide at Jono-Oge due to the 2018 Sulawesi earthquake. Soils and Foundations (Accepted for publication), Indonesia

Kadarusman A, van Leeuwen TM, Sopaheluwakan J (2011) Eclogite, peridotite, granulite, and associated high-grade rocks from The Palu region, central Sulawesi, Indonesia: an example of mantle and crust interaction in a young orogenic belt. Proceedings of JCM Makassar

Kishida H (1966) Damage to reinforced concrete buildings in Niigata city with special reference to foundation engineering. Soils Found 6(1):71–88. https://doi.org/10.3208/sandf1960.6.71

Kiyota T, Furuichi H, Hidayat RF, Tada N, Nawir H (2020) Overview of long-distance flow-slide caused by the 2018 Sulawesi earthquake, Indonesia. Soils Found. https://doi.org/10.1016/j.sandf.2020.03.015

Kokusho T (1999) Water film in liquefied sand and its effect on lateral spread. J Geotechn Geoenviron Eng 125(10):817–826. https://doi.org/10.1061/(ASCE)1090-0241(1999)125:10(817)

Kokusho T (2015) Major advances in liquefaction research by laboratory tests compared with in-situ behavior. Soil Dyn Earthq Eng 91:3–22. https://doi.org/10.1015/j.soildyn.2015.07.024

Kokusho T, Kojima T (2002) Mechanism for post liquefaction water film generation in layered sand. J Geotech Geoenviron Eng 128(2):129–137. https://doi.org/10.1061/(ASCE)1090-0241 (2002)128:2(129)

Mason B, Gallant A, Hutabarat D, Montgomery J, Reed A, Wartman J, Irsyam M, Prakoso W, Djarwadi D, Harnanto D, Alatas I, Rahardjo P, Simatupang P, Kawanda A, Hanifa R (2019) Geotechnical reconnaissance: the 28 September 2018 M7.5 Palu-Donggala, Indonesia Earthquake, GEER association Report No. GEER-061. https://doi.org/10.18118/G63376

National Agency of Disaster Management (2018) Gempa Bumi Sulteng: Retrieved 12 Nov 2018. https://bnpb.go.id/geoportal.html

Okamura M, Ono K, Arsyad A, Minaka US, Nurdin S (2020) Large scale flow-side in Sibalaya caused by the 2018 Sulawesi earthquake. Soils Found 59(5):1148–1159

Socquet A, Hollingsworth J, Pathier E, Bouchon M (2019) Evidence of supershear during the 2018 magnitude 7.5 Palu earthquake from space geodesy. Nature Geosci 12:192–199

U.S. Geological Survey (2019) M 7.5–70 km N of Palu, Indonesia. Retrieved 22 March 2019, from https://earthquake.usgs.gov/earthquakes/eventpage/us1000h3p4/map

van Leeuwen TM (2005) Stratigraphy and tectonic setting of the Cretaceous and Paleogene volcanic-sedimentary successions in northwest Sulawesi, Indonesia: implications for the Cenozoic evolution of western and northern Sulawesi. J Asian Earth Sci 25:481–511

Watkinson MI (2011) Ductile flow in the metamorphic rocks of central Sulawesi, the SE Asian gateway: history and tectonics of the Australia-Asia collision 355:157–176